Double-pulse machining as a technique for the enhancement of material removal rates in laser machining of metals

A. C. Forsman,[a] P. S. Banks, M. D. Perry, E. M. Campbell, A. L. Dodell, and M. S. Armas
General Atomics, Photonics Division, 10240 Flanders Court, San Diego, California 92121-2901

(Received 18 April 2005; accepted 14 June 2005)

Several nanosecond 0.53-μm laser pulses separated by several tens of nanoseconds have been shown to significantly enhance (three to ten times) material removal rates while minimizing redeposition and heat-affected zones. Economic, high-quality, high-aspect ratio holes (>10:1) in metals are produced as a result. A phenomenological model whereby the second laser pulse interacts with the ejecta produced by the first laser pulse and in close proximity to the material surface is consistent with the observations. Incident laser wavelengths of 1.05 and 0.35 μm also benefit from this pulse format. © *2005 American Institute of Physics*. [DOI: 10.1063/1.1996834]

I. INTRODUCTION

The fabrication of high-quality, large-aspect ratio (>10:1) holes is motivated by a variety of applications, ranging from the manufacturing of oil gallery holes[1] in engine blocks to the milling of explosives by femtosecond laser systems.[2] Pulsed lasers having a wide range of pulse durations and repetition rates have been used to fabricate high-aspect ratio slots and holes,[3] and it is these structures that are the focus of this research.

A frequently observed and undesirable trend in laser processing is that material redeposits on the bore walls of the holes being drilled, producing a heat-affected zone resulting from thermal conduction from the ablation plasma and from hot redeposited ejecta. Additionally, there is a tendency for the laser drilling process itself to stall due to laser interaction with the ejecta and redeposition of the ejecta and thereby encounter limits in depth and aspect ratio.[4]

At one extreme of laser technology, picosecond and femtosecond lasers deposit their energy in the skin depth of conductors in such short times that the target material is heated and then ablates due to the immense thermal pressure developed, and this process happens on a time scale too short for significant thermal conduction to lead to significant energy transport. Ultrashort pulse machining therefore relies on having a laser-pulse duration that is too short for an ablation plasma to form during the laser pulse. Such short pulse lasers have been shown to produce high-quality holes in numerous conductors.[2] However, the small amount of material removed per pulse (approximately skin depth in metals, $\leqslant 1$ μm in insulators and semiconductors), the need for reduced pressure or helium atmosphere due to the high irradiance ($>10^{13}$ W/cm^2) on the sample, and the cost of the system have limited the commercial use of these systems.[2,5]

The modern generation of short-pulse Q-switched solid-state industrial lasers, having pulse lengths ranging from 3 to 200 ns, places two additional tools at the disposal of the process designer. First, the high peak power (>10 kW) allows for efficient frequency up conversion, enabling the process designer to more easily take advantage of the greater penetrating power of the shorter wavelengths, such as 0.53, 0.35, and 0.26 μm, owing to the higher critical electron densities ($n_{\mathrm{crit}} \approx 10^{21}/\lambda^2 e^-/\mathrm{cc}$) which accompany the shorter wavelengths.[6] Also, as is well known, the shorter laser pulse in itself deposits more energy in the solid target before substantial interaction with the plasma and evaporated material prevents direct deposition. Auxiliary processes, such as high-pressure gas assist jets, are widely used to clear away melt and vapors, thereby improving the ability of the laser light to reach the target surface.[7]

The motivation in the above methods is to preserve, as much as possible, the ability of the laser light to reach and deposit energy directly in the solid target material rather than plasma, target vapor, melt, or other debris ejected from the target due to rapid laser heating. The present paper discusses a method by which instead of trying to reduce the presence of the target debris in the vicinity of the target point, a secondary laser pulse can be timed to use the debris to great advantage. This process is distinct from a previous work involving a long pulse followed by a short pulse[8] that was designed to first produce a pool of melt and then use high laser-induced pressure to drive the melt away from the target. The process described in this paper does not rely on the presence or absence of a pool of melt, and the secondary pulse interaction does not appear to be dominated by the interaction with the macroscopic pool of molten target material. The available data do not indicate whether the ejected debris contains microscopic molten droplets. High-quality "femtosecond-class" holes but with favorable economics are possible with this approach.

II. DOUBLE NANOSECOND PULSES: CONDITIONS PRODUCED BY THE FIRST PULSE

Figure 1 shows a pulse format typical of the present work, Fig. 2 shows the enhancement in material removal rates, in μm/pulse, for both steel and aluminum, and Fig. 3 shows the enhancement in quality in percussion drilling that is afforded by using a double-pulse technique in stainless

[a]Electronic mail: forsma@gat.com

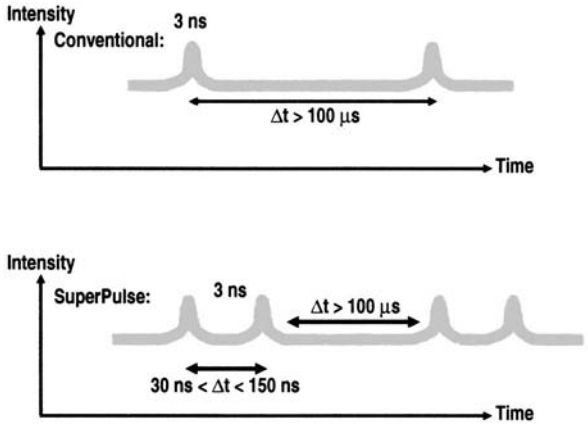

FIG. 1. Conventional and superpulse formats for stainless steel, aluminum, and silicon. This schematic drawing compares the conventional pulse format with the superpulse format. The times used to rate range from 100 μs to 100 ms between the single pulses of the conventional technique or between the pairs of pulses of the superpulse technique, and from 30 to 150 ns between the pair of pulses of the superpulse technique. The fluences tested range from 20 to 200 J/cm^2, and peak irradiances are from 0.7 to 7 GW/cm^2.

steel. It was found empirically that pulse delays less than 30 ns (in normal atmosphere) compromised the benefit, and that increasing the delay beyond 30 ns, up to 90 ns, did not increase the benefit further. Additional tests show that the benefit degrades for delays greater than 150 ns for percussion drilling in type-304 stainless steel. Similar increases in machining efficiency have also been observed in 50-μm-thick steel samples, and in various thicknesses (<2 mm) of tungsten, rhenium, and titanium. These various samples of material, in various thicknesses, have been tested to determine the material effects on the removal process, and to explore the dependence of drilling efficiency on the material properties. All the drilling tests reported in this paper have been conducted using a 532-nm laser light.

From the viewpoint of understanding the nature of a double-pulse interaction, insight was provided by the dependence of the double-pulse drilling efficiency on hole depth. The drilling enhancement for holes drilled through 50-μm-thick stainless steel was approximately the same as the enhancement observed in 1-mm-thick samples of stainless steel. However, no enhancement was observed in 50-μm-thick samples of aluminum but as shown in Fig. 2, substantial enhancement was observed in 1-mm-thick samples of aluminum. This suggests that at least two mechanisms for enhancement play a role, and a phenomenological model to account for this behavior follows.

In order to explain the mechanisms by which the double-pulse enhances laser drilling, the laser-matter interaction physics was investigated. Figure 4 shows the experimental diagnostics that were deployed in these experiments.

A velocity interferometer system for any reflector[9] (VISAR) was used to estimate the pressure generated by the laser. The 3-ns laser pulses, focused into a 100-μm diameter spot, were used to drive pressure waves through 10-μm-thick aluminum foil, thus providing the basis for the assumption of planar geometry in interpreting the results.[10] Aluminum was chosen for its well known equation of state and high sound speed. The pressure wave initiated by laser ablation would

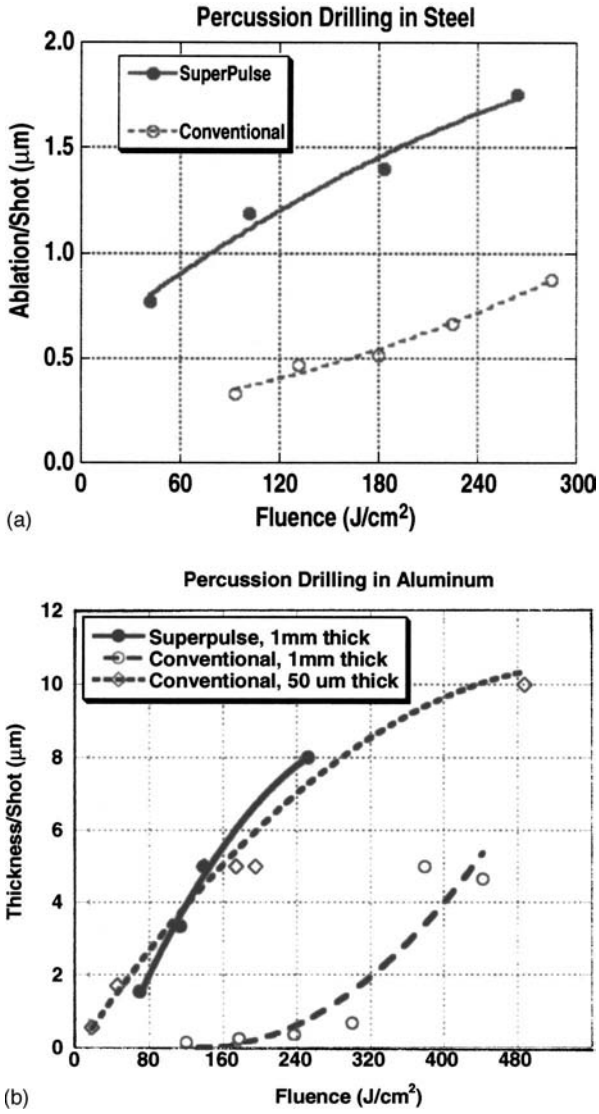

FIG. 2. (a) Percussion drilling rates in steel and (b) drilling rates in aluminum. The figures show the percussion drilling rates in steel and aluminum measured by dividing the piercing time by the number of shots fired. This graph shows that the enhancement gained by double-pulse drilling is substantial for thick steel and thick aluminum samples (hole aspect ratio >10:1), but not for thin aluminum samples (hole aspect ratio <1:1). The enhancement for drilling in thin steel is approximately the same as the enhancement gained by using the double-pulse technique in thick steel, but is not shown here for reasons of clarity. These data were gathered using a 50-μm focal spot, f:10 optics, and a 532-nm laser in normal atmospheric conditions.

take approximately 2 ns to traverse the foil,[11] which is less than the duration of the laser pulse. Thus, rarefaction waves would not have an opportunity to set in and the VISAR would sample the peak ablation pressure. Hence, when the pressure wave arrives at the back of the foil and causes the surface to accelerate and the acceleration is subsequently recorded by the VISAR the pressures inferred from the velocity measurements would reflect the ablation pressure. The pressure is derived according to the formula[12]

$$P = \rho\left(\frac{V_{\mathrm{rel}}}{2}\right)\left(a\frac{V_{\mathrm{rel}}}{2} + C_S\right), \tag{1}$$

where ρ is the mass density, V_{rel} is the release velocity measured by the VISAR, C_S is a constant (5.4×10^3 m/s),

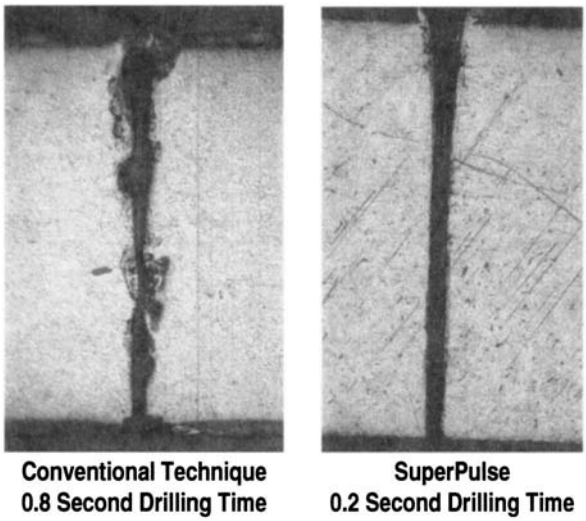

FIG. 3. Enhancement in quality due to superpulse. The figure compares the hole qualities obtained in percussion drilling 40-μm diameter holes through 914-μm-thick 304 stainless steel with a 533-nm laser light. In this test, the conventional technique was implemented using a laser system that fired 10 000 pulses/s, where each pulse had an energy of 2.4 mJ and a duration of 4 ns. The superpulse technique was implemented using a laser system firing 10 000 superpulses/s, where the primary and secondary components of each superpulse contained 1.2 mJ and had a duration of 4 ns and a separation of 70 ns. Thus, each superpulse contained 2.4 mJ, as did the conventional pulses. Therefore, in terms of fluence and firing rate this set of data is a direct comparison of superpulse and conventional techniques. The samples were not subjected to postprocessing techniques such as acid etching and no gas assists were used.

roughly equal to the sound speed, P is the pressure, and the coefficient a is equal[13] to 1.34.

The foil was an unpolished rolled aluminum foil;[14] however, provided the reflectivity and surface structure of the foil do not undergo significant changes on the 3-ns time scale of the probe laser, the absolute reflectivity of the foil is not

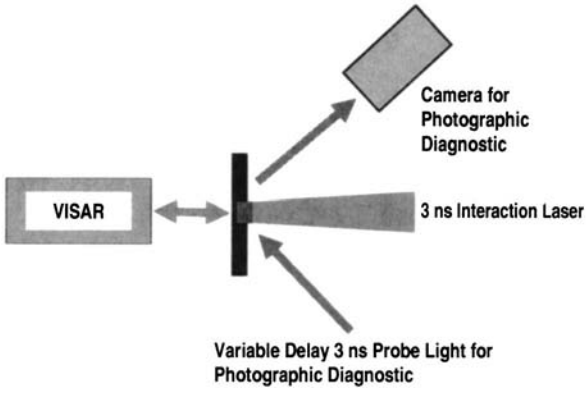

FIG. 4. *In situ* experimental diagnostics. The figure schematically shows the application of two diagnostic techniques to the interaction of the primary pulse with a 10-μm-thick aluminum target. One diagnostic consists of an obliquely incident pulse probe laser illuminating the interaction zone of the target, and the reflected probe light is imaged onto a camera. This diagnostic thus photographs the target surface at various times during and after the interaction laser strikes the target. The second diagnostic is a velocity interferometer system for any reflector (VISAR). It is used to measure the acceleration imparted to the rear surface of the 10-μm target foil by the pressure wave induced by the laser-driven ablation of the front surface of the target by the interaction laser. The VISAR was used to measure the acceleration induced by both the primary and secondary pulses.

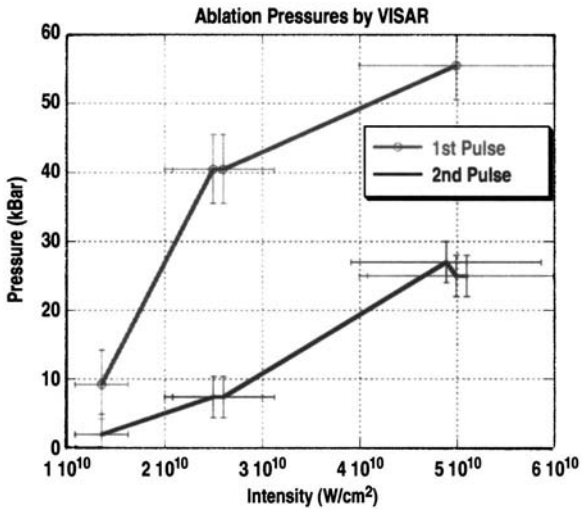

FIG. 5. Pressures produced by the primary and secondary laser pulses. The figure shows the pressures generated by the primary and the secondary laser pulses, for a pulse separation of 50 ns.

needed for the interpretation of the VISAR results. Given the modest shock wave pressures involved, it is unlikely that the surface condition would change significantly[15] within the 3-ns duration probe-laser pulse.

A further consideration is whether or not the same assumption of one-dimensional motion of the target rear surface that was made for interpreting the arrival of the pressure wave induced by the primary laser pulse may be made for the arrival of the secondary laser pulse. The validity of this assumption may be gauged by the magnitude of the surface motion that could occur between the primary and secondary laser pulses in the 90-ns interpulse interval. The maximum surface velocities measured by the VISAR was less than 500 m/s; therefore the maximum surface motion was 45 μm, and this corresponds to the highest laser intensity used in the experiment (shown in Fig. 5). The surface motion that would be expected for the lower-intensity laser pulses would only be of the order of 10 μm. These calculated movements do not take mechanical factors, such as the energy required to stretch the foil, into account and therefore represent a worst-case estimate. A related observation is that there were no cases where penetration of the foil by the laser light was observed for either the primary or the secondary pulse. However, postshot examination of foil samples subjected to a primary laser pulse only did show complete penetration. This indicates that the foil was still in motion when the secondary pulse struck the foil.

Clearly, the assumption of one-dimensional motion for probing secondary shock wave pressures is weaker in the case of the high-intensity laser pulses than it is for the low-intensity laser pulses. However, there are two mitigating factors. The first is that, as previously discussed, since the duration of the driving pulse is longer than the shock wave transit time through the foil, the foil that is not ablated by the laser will be accelerated. Combined with the inference that the foil is still moving when the secondary laser pulse strikes, this suggests that the irradiated region is not subject to 45-μm-deep distortions, but is a region of foil displaced by

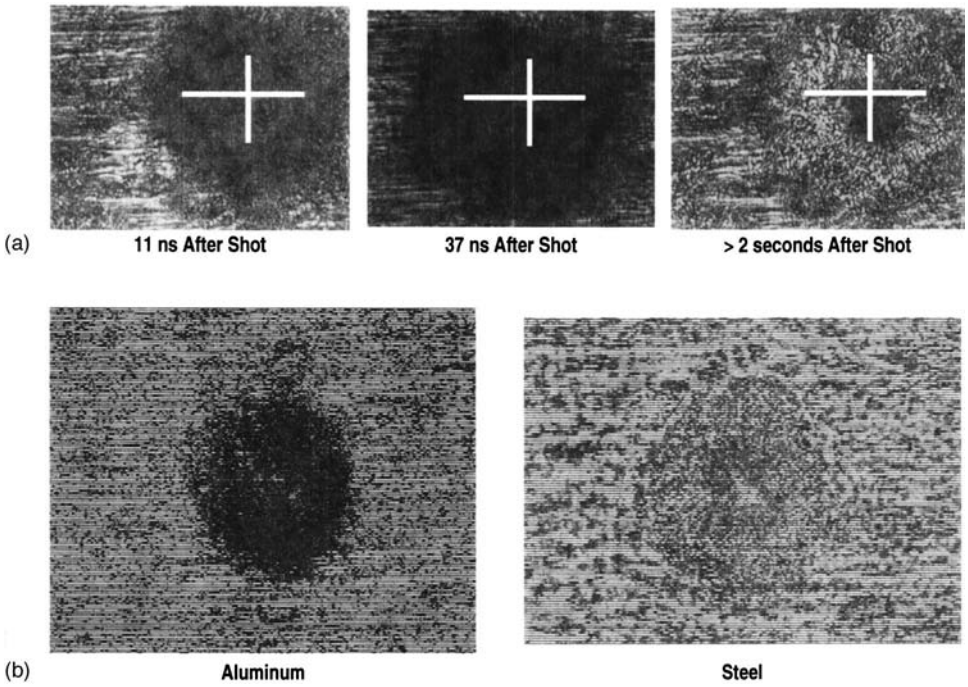

FIG. 6. (a) Photographs of an aluminum target at different times following a single-pulse 100-μm diameter laser strike. The field of view is approximately 150 μm. (b) Comparison of the ejecta produced by aluminum and steel targets following a single-pulse laser strike. (a) shows the evolution of the ejecta above the target. The left-hand picture shows the obscuration of the target surface by the ablation plasma. The target surface is identifiable by the striations imprinted on the surface of the rolled aluminum target. These striations are visible only on one side of the picture at early times, on both sides of a ejecta at intermediate times (central picture), and the entire damage spot is visible when the postshot reference image was recorded (right-hand picture). (b) compares the ejecta produced by a laser strike on an aluminum target with that of a steel target 200 ns after the laser strike. Whereas the aluminum target ejecta still obscures the surface of the aluminum target, the features of the steel target are becoming visible through the ejecta.

45 μm and may have smaller distortions due to focal spot nonuniformities superimposed for high intensities. Given that the maximum focal spot nonuniformity was approximately 30%, the maximum rear surface distortions should be, again ignoring mechanical processes such as stretching, of the order of 10 μm. Since the VISAR is sampling the foil over a 3-ns time period that follows the secondary laser pulse, it is the distortions in the shape of the surface that matter, not the 45-μm shift in the average position of the surface. The 10-μm distortions are small compared to the 100-μm focal spot diameter.

The second mitigating factor is that the data of greatest interest lie in the medium- and low-intensity ranges of Fig. 5, since when using $f:10$ optics this is what correspond to the pulse energies available with diode-pumped solid-state (DPSS) lasers used in micromachining. In these cases, rather than having 10-μm distortions superimposed upon a surface displaced by 45 μm, one would expect to have small distortions superimposed on a surface displaced by less than 20 μm.

Figure 5 shows the pressures produced by the primary and secondary laser pulses. The lower pressures of the secondary laser pulse indicate that the secondary laser pulse does not strike the solid target material. If it had, then the pressure produced by the primary and secondary laser pulses would be similar. Another possibility that deserves consideration is that the secondary laser pulse strikes a layer of molten aluminum lying on top of the target. However, since molten aluminum has only a slightly lower sound speed than solid aluminum,[16] a direct laser strike on a layer of liquid aluminum in contact with the underlying target material would produce a pressure in the solid target that is higher than the pressure in the liquid portion due to the slight impedance mismatch[12] at the liquid-solid interface. Because the enthalpy of melting is only 5% of the enthalpy of vaporization the ablation process should not be appreciably changed by starting on a molten surface, as opposed to a solid surface, and therefore the initial pressure wave in a pool of liquid aluminum produced by a direct laser strike would be approximately equal to that produced in a solid aluminum target. Consequently, the secondary laser pulse could not have struck a layer of molten aluminum lying on top of the target since it would have produced a shock pressure at the backside similar to or greater than that produced by the primary laser pulse.

Photographic measurements of the target surface for times immediately after an interaction pulse has impacted show the evolution of a cloud of ejecta in front of the target. These photographs were taken using a low-intensity nanosecond laser pulse as a variable-delay probe to illuminate the target at different times following the interaction laser pulse, as shown in Fig. 4. The interaction pulse was pure 355 nm and the probe pulse was pure 532 nm. The reflected probe light was then imaged onto a camera using $f:3$ optics. Figure 6 shows a series of photographs taken a different times following the exposure of a l-mm-thick aluminum target to a 3-ns interaction pulse having an intensity of $\sim 4 \times 10^{10}$ W/cm^2. The evolution of the ejecta produced by the laser pulse is evident, and the photographs show that the ejecta screens the surface of one side of the target point from

view for times <37 ns but that at later times a cloud of ejecta obscures only the target point. It is unclear from this data whether the mechanism of obscuration is absorption or refraction. However, the empirically determined optimum delay times coincide with the presence of the ejecta that obscures only the target point, and hence the secondary laser pulse strikes the ejecta.

III. DOUBLE NANOSECOND PULSES: A PHENOMENOLOGICAL MODEL

A four-step model is proposed to account for the improved material removal afforded by a double-pulse technique. In the first step, the primary laser pulse produces a plasma and other ejecta in front of the target.

The second step is the delay period between the primary and secondary laser pulses. During this period, that has been typically between 40 and 150 ns for experiments conducted in air, the plasma dissipates but other ejecta remain over the target point.

The third step is the heating of the ejecta by the secondary laser pulse as discussed above. The relatively low pressure produced by the secondary pulse shows that the secondary pulse does not strike the target surface directly otherwise the secondary pressure would at least be equal to the primary pressure since the irradiance is similar. It is asserted in this simple model that the secondary laser pulse is absorbed within the volume of the ejecta that has lingered in front of the target following the primary pulse. The choice of this assertion rests on the pressure measurements: if the secondary laser pulse were absorbed predominantly at the outside of the ejecta, then the release pressure wave (which is measured at the back target surface) would probably be unobservable. In this model, the ejecta is presumed to be at a fraction of solid density and so the sound speed through the ejecta would be significantly less than the solid Al target. Consequently, having to propagate a pressure wave through, for example, 10 μm of ejecta would take several times as long as propagating a pressure wave through the 10-μm target. Since the VISAR recorded a pressure wave arriving at the back target surface 2 ns after both the primary and secondary laser pulses then the secondary laser pulse had to affect the front target surface within 1 ns of its arrival, just as the primary pulse did. The simple model is thus to assume that the secondary pulse is absorbed within the volume of the ejecta, and the heated ejecta now applies pressure to the target surface.

The fourth step is the ablation of the target material by the heated ejecta. However, the process of ablation by the heated cloud of ejecta is more efficient than ablation by the primary pulse direct strike due to the lower pressure that accompanies the secondary pulse. The simple model states that the primary laser pulse ablates the material since thermal conduction transports energy from the critical density layer to the solid target material, but that ablation is restrained by the pressure that accompanies this process. The secondary laser pulse provides a thermal heat source in contact with the target by heating the ejecta, but with only a fraction of the pressure so that mass removal may proceed more efficiently.

This four-step model needs to be slightly modified to account for the different behaviors of steel and aluminum. Using a double-pulse technique provides roughly the same enhancement in drilling speed in both 50-μm and 1-mm samples of steel, thus reinforcing the idea that it is the modification of the ablation process that is responsible for the increase in machining speed. Using a double-pulse technique in aluminum provided no enhancement in <500-μm-thick aluminum samples but provided a tremendous enhancement in 1-mm-thick samples for the pulse separations studied. The simple model can be modified using the photographs of Fig. 6 as a guide, which show aluminum targets producing ejecta that obscures the underlying target for longer periods of time than steel targets. Again, a simple interpretation is that the aluminum ejecta is more massive and when heated by the secondary laser pulse it is more likely to expand out of a hole than if only a single pulse were used. For shallow holes (thin targets) the aluminum ejecta clears the hole even in the absence of a secondary laser pulse and hence no enhancement in machining speed is noted.

There are two mechanisms by which heating the ejecta by a secondary pulse acts then. One is to provide an efficient mechanism for ablation, and the other is to heat the ejecta so that hole occlusion is reduced and heated ablated material is not redeposited. The first mechanism is dominant when the ejecta is sufficient to absorb the laser light but not sufficient to hinder efficient thermal conduction to the target surface, and the second mechanism dominates when the ejecta is sufficient to both absorb the laser light and inhibit thermal conduction to the target surface.

IV. CONCLUSION

A pulse format that improves the machining speed through efficient ablation and that extends the capability of percussion drilling small, high-aspect ratio holes in certain materials by reducing hole occlusion rates has been developed. A simple model to provide a framework within which the data produced by the double-pulse format may be interpreted has been proposed.

ACKNOWLEDGMENT

This work was done with the corporate support of General Atomics.

[1] H. Rohde, in *LIA Handbook of Laser Materials Processing*, edited by J. F. Ready (■, ■, 2001), pp. 474–477.
[2] M. D. Perry, B. C. Stuart, P. S. Banks, M. D. Feit, and J. A. Sefcik, in *LIA Handbook of Laser Materials Processing*, edited by J. F. Ready (■, ■, 2001), pp. 499–508.
[3] *LIA Handbook of Laser Materials Processing*, edited by J. F. Ready (■, ■, 2001), Chaps. 12 and 13.
[4] D. Bäuerle, *Laser Processing and Chemistry* (Springer, Berlin, 2000), p. 244.
[5] G. Thomas, J. T. Schriempf, and R. Gilmore, Proc. SPIE **4977**, 108 (2003).
[6] B. Meyer *et al.*, Phys. Fluids **27**, 302 (1984); F. Cottet *et al.*, Phys. Rev. Lett. **52**, 1884 (1984); S. I. Anisimov *et al.*, Usp. Fiz. Nauk **142**, 395 (1984) [Sov. Phys. Usp. **27**, 181 (1984)].
[7] J. Fieret, M. J. Terry, and B. A. Ward, Proc. SPIE **668**, 53 (1986).
[8] C. Lehane and H. S. Kwok, Appl. Phys. A: Mater. Sci. Process. **73**, 45 (2001).
[9] A. C. Forsman and G. A. Kyrala, Phys. Rev. E **63**, 056402 (2001).
[10] S. I. Anisimov *et al.*, Usp. Fiz. Nauk **142**, 395 (1984) [Sov. Phys. Usp. **27**, 181 (1984)].

[11]*CRC Handbook of Chemistry and Physics*, 78th ed., edited by D. R. Lide (CRC, New York, 1998).
[12]Y. B. Zeldovich and Y. P. Raizer, *Physics of Shock Waves and High Temperature Hydrodynamic Phenomena*, edited by W. D. Hayes and R. F. Probstein (Dover, New York, 2002).
[13]A. C. Mitchell and W. J. Nellis, J. Appl. Phys. **52**, 3363 (1981).
[14]GoodFellow Cambridge, Ltd., Huntingdon, England.
[15]M. Werdiger *et al.*, Laser Part. Beams **547**, 17 (1999).
[16]J. R. Asay and D. B. Hayes, J. Appl. Phys. **46**, 4789 (1975).